The atypical chemokine receptor 2 limits renal inflammation and fibrosis in murine progressive immune complex glomerulonephritis

Andrei Bideak[1], Alexander Blaut[1], John M. Hoppe[1], Martin B. Müller[1], Giuseppina Federico[2], Nuru Eltrich[1], Hermann-Josef Gröne[2], Massimo Locati[3,4] and Volker Vielhauer[1]

[1]*Nephrologisches Zentrum, Medizinische Klinik und Poliklinik IV, Klinikum der Universität München, Ludwig-Maximilians-University Munich, Munich, Germany;* [2]*Department of Cellular and Molecular Pathology, German Cancer Research Center, Heidelberg, Germany;* [3]*Humanitas Clinical and Research Center, Rozzano, Italy; and* [4]*Department of Medical Biotechnologies and Translational Medicine, Università degli Studi di Milano, Milan, Italy*

The atypical chemokine receptor 2 (ACKR2), also named D6, regulates local levels of inflammatory chemokines by internalization and degradation. To explore potential anti-inflammatory functions of ACKR2 in glomerulonephritis, we induced autologous nephrotoxic nephritis in C57/BL6 wild-type and *Ackr2*-deficient mice. Renal ACKR2 expression increased and localized to interstitial lymphatic endothelium during nephritis. At two weeks Ackr2$^{-/-}$mice developed increased albuminuria and urea levels compared to wild-type mice. Histological analysis revealed increased structural damage in the glomerular and tubulointerstitial compartments within Ackr2$^{-/-}$ kidneys. This correlated with excessive renal leukocyte infiltration of CD4^{+} T cells and mononuclear phagocytes with increased numbers in the tubulointerstitium but not glomeruli in knockout mice. Expression of inflammatory mediators and especially markers of fibrotic tissue remodeling were increased along with higher levels of ACKR2 inflammatory chemokine ligands like CCL2 in nephritic Ackr2$^{-/-}$ kidneys. *In vitro*, *Ackr2* deficiency in TNF-stimulated tubulointerstitial tissue but not glomeruli increased chemokine levels. These results are in line with ACKR2 expression in interstitial lymphatic endothelial cells, which also assures efflux of activated leukocytes into regional lymph nodes. Consistently, nephritic Ackr2$^{-/-}$ mice showed reduced adaptive cellular immune responses indicated by decreased regional T-cell activation. However, this did not prevent aggravated injury in the kidneys of Ackr2$^{-/-}$ mice with nephrotoxic nephritis due to simultaneously increased tubulointerstitial chemokine levels, leukocyte infiltration and fibrosis. Thus, ACKR2 is important in limiting renal inflammation and fibrotic remodeling in progressive nephrotoxic nephritis. Hence, ACKR2 may be a potential target for therapeutic interventions in immune complex glomerulonephritis.

Correspondence: *Volker Vielhauer, Nephrologisches Zentrum, Medizinische Klinik und Poliklinik IV, Klinikum der Universität München, Ludwig-Maximilians-University Munich, Ziemssenstrasse 1, 80336 Munich, Germany. E-mail: Volker.Vielhauer@med.uni-muenchen.de*

Received 14 April 2017; revised 28 October 2017; accepted 16 November 2017

Kidney International (2018) ■, ■–■; https://doi.org/10.1016/j.kint.2017.11.013

KEYWORDS: chemokine; fibrosis; glomerulonephritis; inflammation

Glomerulonephritis (GN) is a major cause of renal failure worldwide leading to end-stage renal disease.[1] It is often caused by glomerular deposition or *in situ* formation of immune complexes, which trigger adaptive humoral and cellular immune responses toward intrinsic or planted glomerular antigens, renal leukocyte infiltration, and cell-mediated renal damage.[2,3]

Chemokines and their receptors orchestrate leukocyte migration to sites of inflammation.[4,5] The atypical chemokine receptor 2 (ACKR2), previously named D6, belongs to the subfamily of atypical chemokine receptors, which are characterized by promiscuous binding of proinflammatory chemokines and play important roles in the resolution of inflammatory responses.[6–8] Unlike typical chemokine receptors, ACKR2 is unable to induce cell signaling in response to ligand binding, but it regulates local chemokine levels by scavenging, internalizing, and degrading these molecules. ACKR2 is expressed in many parenchymal organs, including barrier tissues such as the skin, gut, lung, and placenta.[9,10] The primary site of ACKR2 expression in resting tissues is lymphatic endothelium.[11] In addition, ACKR2 is expressed in leukocyte subsets including neutrophils and dendritic cells.[7,12] In several disease models, it was shown that ACKR2 limits *in vivo* inflammation, including skin inflammation,[13] myocardial infarction,[14] and systemic infection with *Mycobacterium tuberculosis*.[15] In addition, ACKR2 inhibits tumorigenesis in inflammation-dependent cancer models.[16,17] In contrast, in experimental autoimmune encephalitis and after subcutaneous challenge of ovalbumin-specific T cells, inflammatory activity was reduced in *Ackr2*-deficient mice due to reduced T-cell priming in draining lymph nodes.[18,19] Together, these studies demonstrated that ACKR2 not only plays a central role in the resolution of inflammation due to reduction of local chemokine

concentrations, but by scavenging inflammatory chemokines on lymphatic endothelial surfaces, ACKR2 also facilitates migration of antigen-presenting cells to lymph nodes, ensuring an efficient generation of adaptive immune responses.[20] Currently, there is no published evidence whether ACKR2 controls chemokine-dependent recruitment and activation of macrophages, dendritic cells, and T cells in an inflammatory renal disease such as GN. However, as these cell types contribute to the initiation and progression of GN, ACKR2 may also be a potential regulator limiting inflammatory responses in the kidney.

We hypothesized that *Ackr2* deficiency aggravates renal inflammation and injury in chronic immune complex GN. We tested this hypothesis by inducing autologous nephrotoxic nephritis (NTN), a rodent model of immune complex-mediated, T-cell–dependent progressive GN, in *Ackr2*-deficient mice and characterized their phenotype compared with the phenotype of wild-type control mice. Here, we show for the first time that ACKR2 plays an important role in limiting renal inflammation, injury, and fibrosis during GN by reducing proinflammatory chemokine levels in inflamed kidneys and subsequent leukocyte infiltration into the tubulointerstitial compartment. In addition, our data demonstrate that ACKR2 facilitates adaptive T-cell responses in regional lymph nodes during autologous NTN. Despite its opposing effects on tubulointerstitial inflammation and adaptive local immune responses in the autologous NTN model, we identified ACKR2 as an endogenous regulator primarily limiting renal injury and fibrosis in chronic GN.

RESULTS

ACKR2 expression in nephritic kidneys with autologous NTN

Analysis of mRNA expression levels in normal and nephritic wild-type kidneys at day 14 of NTN revealed induced expression of ACKR2 in inflamed kidneys (Figure 1a). *In situ* hybridization of Ackr2 mRNA combined with immunofluorescence detection of lymphatic vessel endothelial hyaluronan receptor 1 (LYVE-1)-positive lymphatic endothelial cells localized renal ACRK2 expression to the interstitial lymphatic endothelium in nephritic wild-type kidneys, whereas no mRNA transcripts could be detected in *Ackr2*-deficient ($Ackr2^{-/-}$) mice (Figure 1b). These results show that ACKR2 is prominently expressed in lymphatic endothelial cells of nephritic kidneys with NTN.

Ackr2 deficiency deteriorates renal functional parameters in autologous NTN

To investigate the potential role of ACKR2 in controlling renal inflammation in GN, we induced autologous NTN in wild-type and $Ackr2^{-/-}$ mice. At day 14 of NTN, $Ackr2^{-/-}$ mice, compared with wild-type mice, developed significantly increased albuminuria (Figure 2). Consistently, renal function deteriorated more significantly in $Ackr2^{-/-}$ mice, compared with wild-type mice, indicated by higher serum urea levels (Figure 2). Thus, *Ackr2* deficiency significantly aggravated functional parameters of renal injury in autologous NTN.

Ackr2 deficiency increases glomerular and tubulointerstitial injury in autologous NTN

Increased albuminuria suggested more severe glomerular injury in $Ackr2^{-/-}$ mice compared with wild-type mice. This was confirmed by the presence of more severe glomerulosclerosis, more glomerular fibrinoid necrosis, and a reduced number of preserved podocytes in glomeruli of *Ackr2*-deficient mice (Figure 3a to c). Increased podocyte damage was also indicated by reduced glomerular staining of nephrin and reduced renal nephrin mRNA expression in $Ackr2^{-/-}$ kidneys (Figure 3d).

Moreover, tubulointerstitial injury substantially increased in $Ackr2^{-/-}$ mice compared with wild-type mice at day 14 of NTN, with more tubular casts, tubular dilation, and interstitial volume expansion in $Ackr2^{-/-}$ kidneys (Figure 4a to c). This correlated with higher protein expression of the tubular damage marker kidney injury molecule 1 (KIM-1) in $Ackr2^{-/-}$ mice (Figure 4d). Together, *Ackr2* deficiency leads

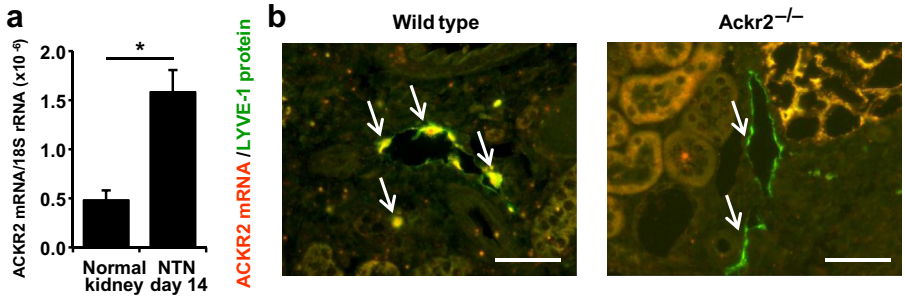

Figure 1 | Renal expression of atypical chemokine receptor 2 (ACKR2) is induced in mice with autologous serum nephrotoxic nephritis (NTN) and localizes to lymphatic vessel endothelial hyaluronan receptor 1 (LYVE-1)-positive lymphatic endothelial cells. (**a**) Ackr2 mRNA levels, normalized to 18S ribosomal RNA (rRNA), in normal murine kidney and in nephritic kidneys at day 14 of NTN. Data represent mean ± SEM; *$P < 0.05$. (**b**) Fluorescence-based *in situ* hybridization of ACKR2 (red) combined with immunofluorescence localization of LYVE-1 (green) demonstrates Ackr2 mRNA expression in LYVE-1–positive interstitial lymphatic endothelial cells (merged yellow signal, indicated by arrows) in nephritic wild-type kidneys at day 14 of NTN (left panel). Ackr2 mRNA expression was not detectable in nephritic kidneys of *Ackr2*-deficient ($Ackr2^{-/-}$) mice (right panel). Images show representative cortical tissue from each group; original magnification ×400, bars = 50 μm. To optimize viewing of this image, please see the online version of this article at www.kidney-international.org.

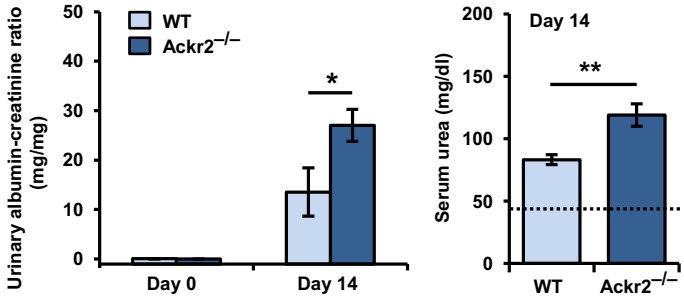

Figure 2 | *Ackr2* deficiency (Ackr2$^{-/-}$) increases albuminuria and renal functional impairment in mice with autologous nephrotoxic serum nephritis. Albuminuria was evaluated in spot urine samples at baseline and day 14 after injection of nephrotoxic serum and is expressed as urinary albumin-creatinine ratio (mg/mg). Serum levels of urea were determined at day 14 of nephrotoxic serum nephritis. The dashed line indicates mean baseline values for normal wild-type (WT) mice. Data are representative for 2 independent experiments and show mean ± SEM of 6 to 8 mice per group. *$P < 0.05$, **$P < 0.01$.

to aggravated functional and structural renal damage in the autologous NTN model of immune complex GN.

Ackr2 deficiency promotes renal leukocyte recruitment in autologous NTN

To investigate whether aggravated renal injury in Ackr2$^{-/-}$ mice correlated with increased renal inflammatory infiltrates, leukocytes were quantified by flow cytometry of renal single-cell suspensions on day 14 of NTN. Flow cytometry revealed a significant increase in CD45^{+} leukocytes in nephritic kidneys of Ackr2$^{-/-}$ mice compared with wild-type mice. CD3^{+} T cells, with increased accumulation of CD4^{+}, but not CD8^{+} T cells, and particularly CD11c^{+} and F4/80^{+} mononuclear phagocytes, were more abundant in kidneys lacking ACKR2 (Figure 5a). We further investigated this result compartment-specifically by immunohistochemistry of cortical renal tissue. Despite increased glomerular damage in Ackr2$^{-/-}$ mice glomerular accumulation of Mac2^{+} macrophages and CD3^{+} T cells was comparable to accumulation in wild-type mice (Figure 5b and c). In contrast, tubulointerstitial infiltration of F4/80^{+} mononuclear phagocytes and CD3^{+} T cells was significantly more abundant in Ackr2$^{-/-}$ mice (Figure 5d and e). Thus, impaired renal functional parameters and more severe renal injury in *Ackr2*-deficient mice were associated with increased interstitial, but not glomerular leukocyte infiltration in NTN.

Ackr2 deficiency increases renal expression of inflammatory markers and fibrosis in autologous NTN

Next, we analyzed renal mRNA expression of proinflammatory mediators in wild-type and Ackr2$^{-/-}$ mice at day 14 of NTN (Figure 6). In Ackr2$^{-/-}$ mice, we found a substantial increase in renal expression of CC chemokine receptor 2 (CCR2), being consistent with a more prominent infiltration of CCR2^{+} leukocytes into inflamed kidneys of these mice. Furthermore, *Ackr2*-deficiency resulted in significantly increased expression of renal CC chemokine ligand 2 (CCL2) and interleukin-6 (IL-6) mRNA, and similar trends for CCL5, pro-IL-1β, IL-12β, tumor necrosis factor (TNF), the T-helper-cell-2 cytokine IL-13, and the M1 and M2 macrophage markers inducible nitric oxide synthase and macrophage scavenger receptor 1, respectively (Figure 6). In addition, expression markers of fibrotic tissue remodeling substantially increased, including renal mRNA levels for fibronectin, laminin, procollagen 1, procollagen 4, the fibroblast marker α-smooth muscle actin (α-SMA), and the fibrosis-associated monocytic marker fibroblast-specific protein 1 (Figure 7a). Consistently, immunohistochemistry revealed an increased accumulation of α-SMA^{+} myofibroblasts in the interstitium of *Ackr2*-deficient kidneys (Figure 7b). Therefore, lack of Ackr2 exacerbates not only renal leukocyte infiltration and inflammatory injury in NTN, but it also increases the fibrotic response in inflamed kidneys.

Bone marrow–derived fibrocytes may contribute to fibrotic remodeling in nephritic kidneys.[21,22] As fibrocytes express CCR2,[22] reduced scavenging of its chemokine ligand CCL2 in *Ackr2*-deficient renal tissue could augment fibrocyte migration into diseased Ackr2$^{-/-}$ kidneys. We therefore quantified renal CD45^{+}CD11b^{+}collagen 1^{+} fibrocytes in nephritic kidneys at day 14 of NTN by flow cytometry, which revealed a significant increase in accumulating fibrocytes in Ackr2$^{-/-}$ kidneys (Figure 7c). Moreover, in both wild-type and Ackr2$^{-/-}$ kidneys, most of these fibrocytes expressed CCR2 (Figure 7c). Thus, *Ackr2* deficiency may directly contribute to renal fibrosis through increased CCL2/CCR2-mediated fibrocyte recruitment.

ACKR2 expression in the tubulointerstitial compartment controls proinflammatory chemokine levels in the kidney

To further explore mechanisms of exacerbated NTN in *Ackr2*-deficient mice, we measured CCL2, CCL5, and CXC chemokine ligand 10 (CXCL10) protein levels in lysates of whole kidneys isolated from wild-type and Ackr2$^{-/-}$ mice at day 14 of NTN. We observed significantly increased levels of these chemokines in nephritic kidneys of Ackr2$^{-/-}$ mice (Figure 8a). As higher numbers of accumulating leukocytes may contribute to intrarenal chemokine expression in Ackr2$^{-/-}$ mice, we performed additional *in vitro* experiments with kidney tissue isolated from healthy wild-type and *Ackr2*-deficient mice. Independently of chemokine production by infiltrating leukocytes, stimulation with TNF resulted in

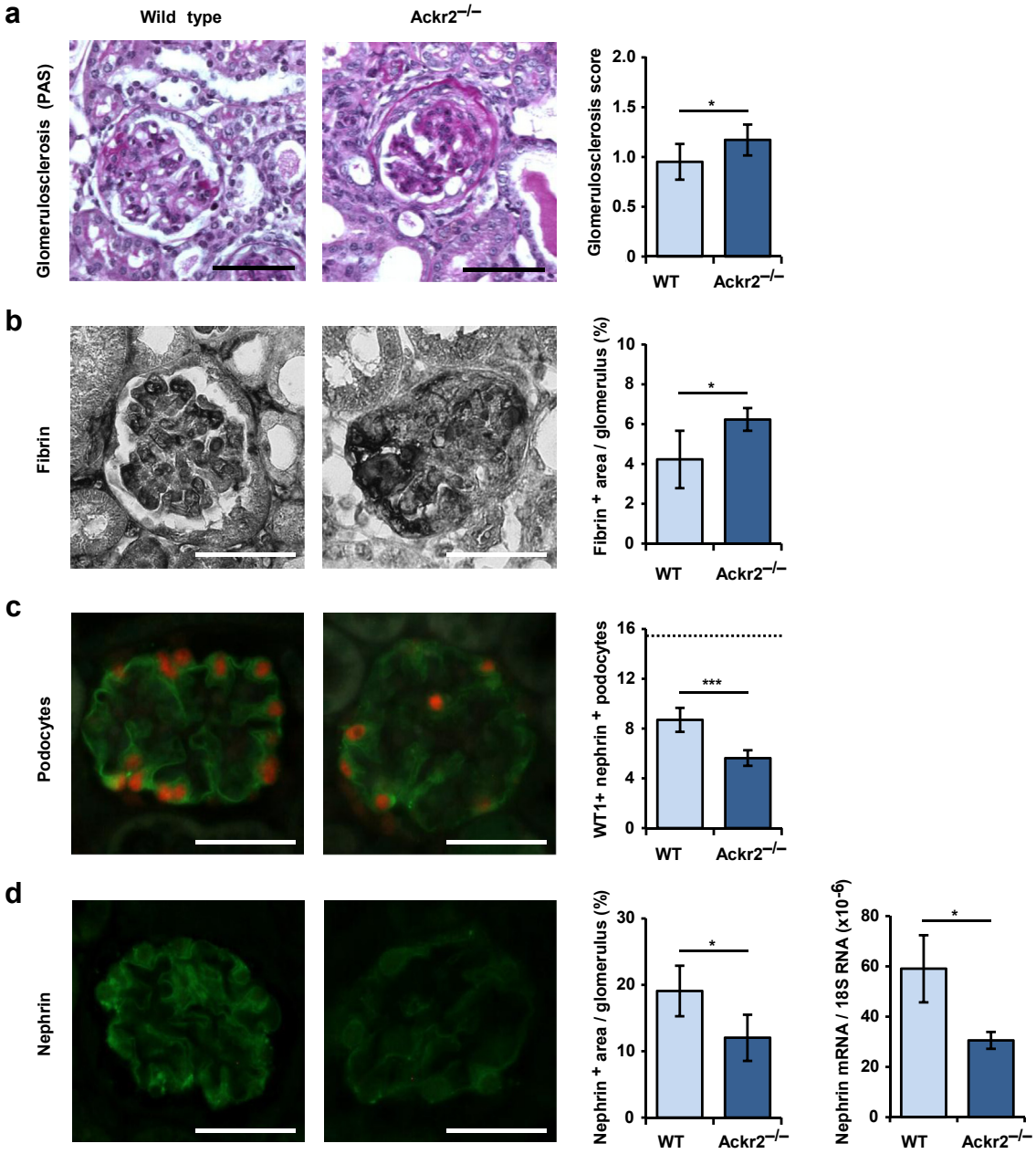

Figure 3 | *Ackr2* deficiency (Ackr2$^{-/-}$) aggravates glomerular injury at day 14 of autologous nephrotoxic serum nephritis. (**a**) Representative photomicrographs of periodic acid-Schiff (PAS)–stained kidney sections from wild-type (WT) and *Ackr2*-deficient mice illustrating glomerular matrix deposition. Semiquantitative scoring revealed more extensive glomerular sclerosis in Ackr2$^{-/-}$ mice. (**b**) Immunohistochemical staining for fibrin demonstrated fibrinoid necrosis in glomeruli of WT mice, which increased in Ackr2$^{-/-}$ mice. (**c**) Podocytes were identified by double staining for nephrin and nuclear Wilms tumor antigen-1 (WT1). Podocyte loss significantly increased in Ackr2$^{-/-}$ mice. The dashed line indicates mean podocyte numbers in healthy WT mice. (**d**) Consistently, immunofluorescence revealed significantly reduced nephrin expression in Ackr2$^{-/-}$ glomeruli compared with WT, and nephrin mRNA expression was lower in Ackr2$^{-/-}$ kidneys. Images show representative glomeruli from each group; original magnification ×400, bars = 50 μm. Semiquantitative and morphometric analysis was performed as described in the Materials and Methods. Data represent mean ± SD of 5 to 6 mice per group. *$P < 0.05$, ***$P < 0.001$. To optimize viewing of this image, please see the online version of this article at www.kidney-international.org.

3.1-fold higher CCL2 levels in supernatants of *Ackr2*-deficient tubulointerstitial cells compared with wild-type tubulointerstitial cells, whereas glomerular CCL2 secretion was not different in the 2 genotypes (Figure 8b). Together with the shown expression of ACKR2 in interstitial lymphatic endothelium (Figure 1), these results are consistent with a reduced degradation of TNF-induced CCL2 by *Ackr2*-deficient lymphatic endothelial cells contained in the tubulointerstitial tissue fraction, but not in the isolated glomerular compartment. Thus, reduced degradation of proinflammatory chemokines in the tubulointerstitium of *Ackr2*-deficient mice leads to increased local chemokine levels and increased

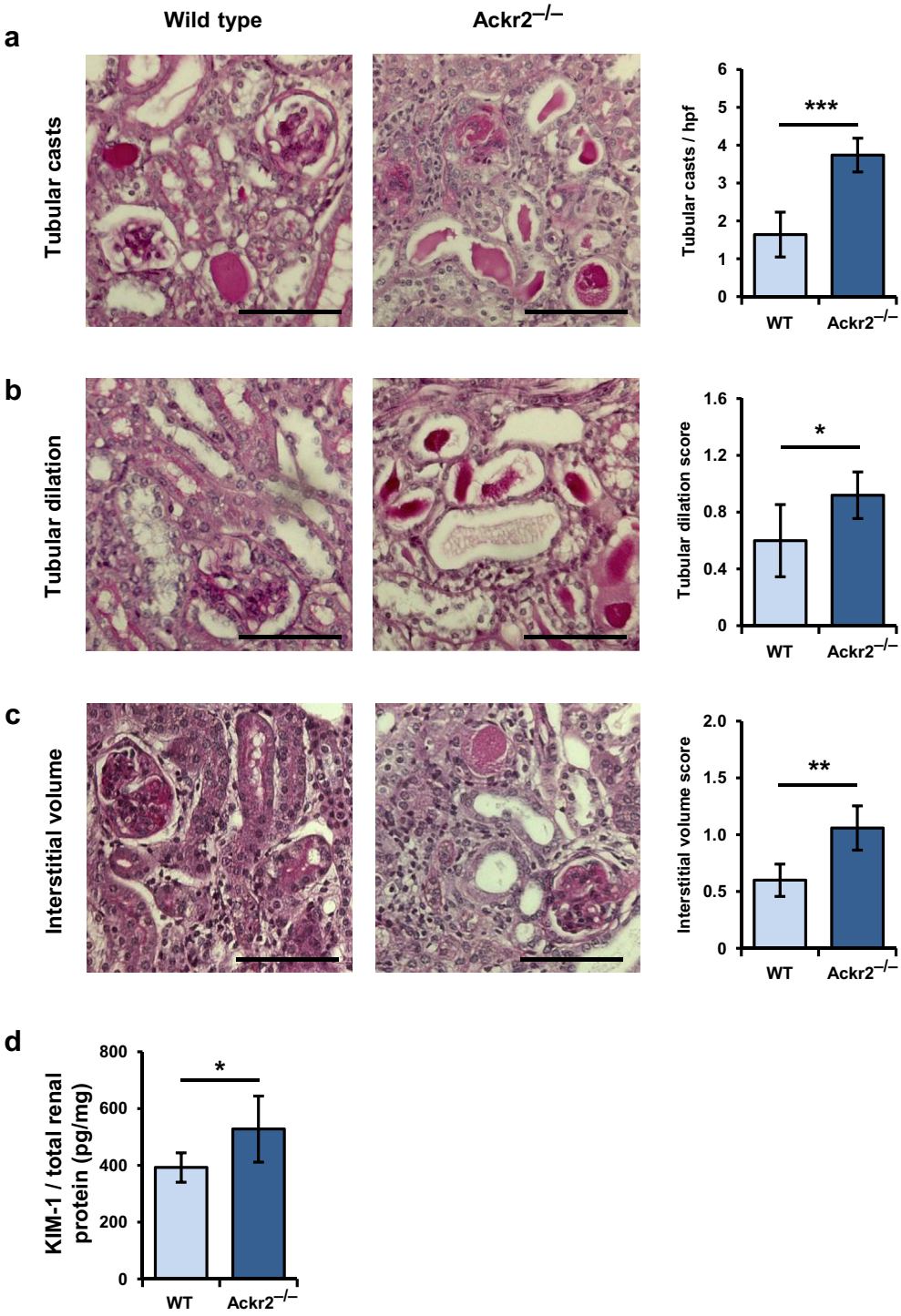

Figure 4 | *Ackr2* deficiency (Ackr2$^{-/-}$) worsens tubulointerstitial injury on day 14 after induction of autologous nephrotoxic serum nephritis. The number of tubular casts (**a**), the extent of tubular dilation (**b**), and interstitial volume expansion (**c**) were significantly increased in Ackr2$^{-/-}$ mice compared with wild-type (WT) control mice. Images show representative tubulointerstitial tissue from each group; original magnification $\times$400, bars = 100 μm. (**d**) Aggravated histological markers of tubulointerstitial injury correlated with an increased protein expression of kidney injury molecule 1 (KIM-1) in *Ackr2*-deficient kidneys, as measured by enzyme-linked immunosorbent assay of kidney lysates. Data represent mean ± SD of 5 mice per group. *$P < 0.05$, **$P < 0.05$, ***$P < 0.001$. hpf, high power field. To optimize viewing of this image, please see the online version of this article at www.kidney-international.org.

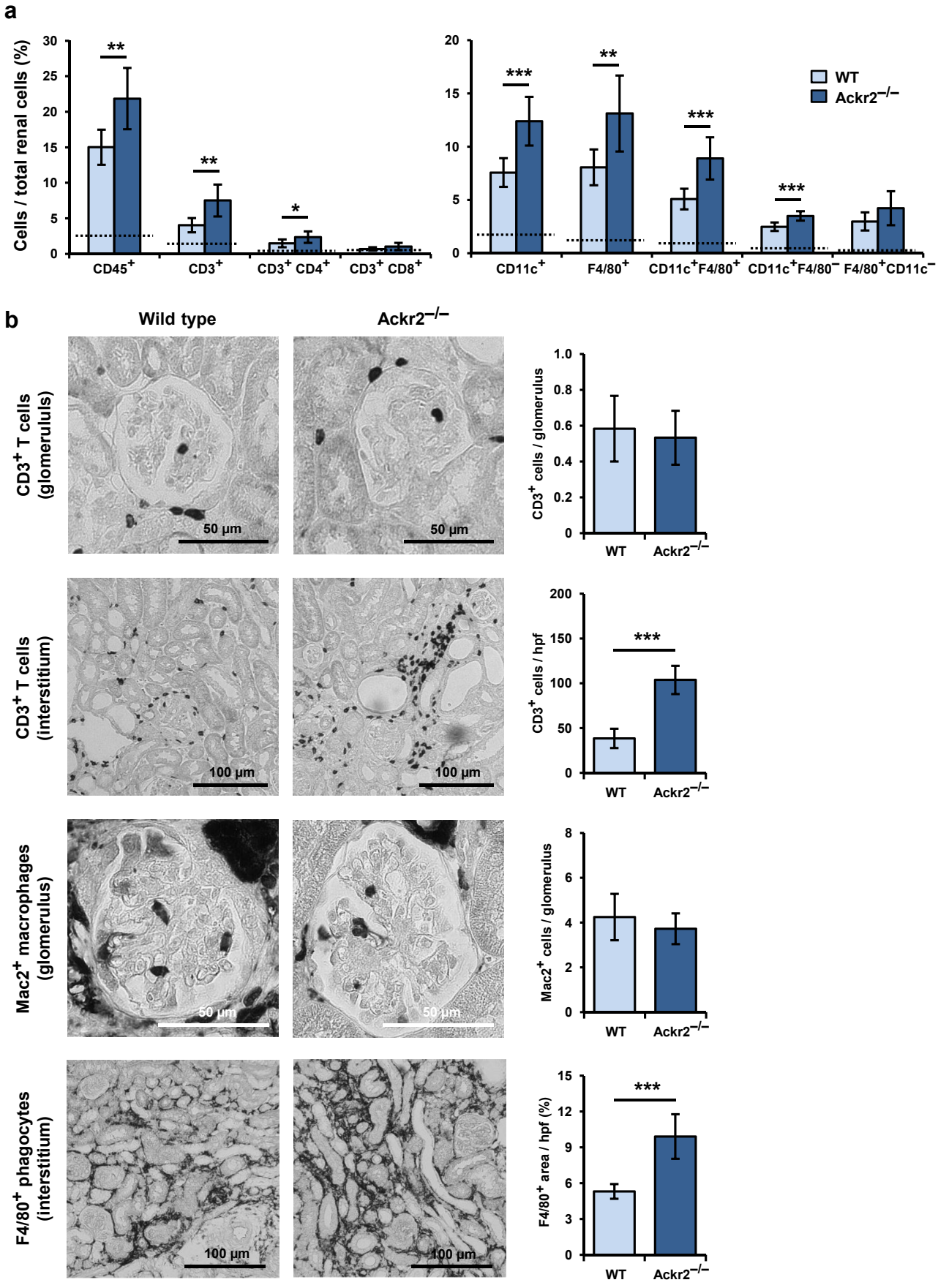
a
Cells / total renal cells (%)
CD45+
CD3+
CD3+ CD4+
CD3+ CD8+
CD11c+
F4/80+
CD11c+F4/80+
CD11c+F4/80−
F4/80+CD11c−
WT
Ackr2−/−
b
Wild type
Ackr2−/−
CD3+ T cells (glomerulus)
CD3+ cells / glomerulus
CD3+ T cells (interstitium)
CD3+ cells / hpf
Mac2+ macrophages (glomerulus)
Mac2+ cells / glomerulus
F4/80+ phagocytes (interstitium)
F4/80+ area / hpf (%)
50 µm
100 µm

tubulointerstitial leukocyte accumulation, which translates into exacerbated inflammation and fibrotic tissue remodeling in Ackr2$^{-/-}$ kidneys during NTN. The predominant tubulointerstitial, but not glomerular effect of *Ackr2* deficiency is in line with the shown parenchymal expression of ACKR2 in interstitial lymphatic endothelial cells.

CCL2 levels and leukocyte counts in peripheral blood increase in *Ackr2*-deficient mice

Next, we investigated potential systemic effects of *Ackr2*-deficiency and measured CCL2 serum levels and peripheral leukocyte counts at day 14 of NTN. CCL2 serum levels were significantly elevated in Ackr2$^{-/-}$ mice (Figure 9a). Moreover, in *Ackr2*-deficient mice, compared to wild-type mice, peripheral leukocyte counts increased, with the most prominent rise evident in inflammatory CD11b^{+}Ly6C^{high} monocytes (Figure 9b). These results are consistent with increased CCR2-dependent monocyte emigration from bone marrow[23,24] mediated by elevated systemic levels of the CCR2 chemokine ligand CCL2 in Ackr2$^{-/-}$ mice. Thus, higher numbers of circulating inflammatory monocytes may additionally contribute to increased renal leukocyte infiltration in *Ackr2*-deficient mice.

Ackr2 deficiency does not affect glomerular and systemic humoral immune responses to the nephritogenic antigen in autologous NTN

As B-cell-dependent humoral immunity contributes to renal injury in autologous NTN,[25] glomerular deposition of autologous murine IgG directed against the planted sheep IgG of the nephrotoxic serum, glomerular complement deposition, and circulating mouse anti-sheep IgG levels were determined in Ackr2$^{-/-}$ and wild-type mice at day 14 of NTN. By histochemistry, glomerular deposition of murine IgG and complement C3d were readily detectable in all mice, without differences between the 2 genotypes (Figure 10a and b). Moreover, serum titers of autologous mouse anti-sheep IgG were not statistically different between Ackr2$^{-/-}$ and wild-type mice (Figure 10c). These data indicate that aggravated renal damage does not result from enhanced humoral immune responses in *Ackr2*-deficient mice.

Ackr2 deficiency attenuates regional T-cell immune responses in autologous NTN

Absence of ACKR2 on lymphatic endothelial cells results in inappropriate inflammatory leukocyte accumulation around lymphatic endothelium and reduced migration of activated cells to draining lymph nodes.[20] As a consequence Ackr2$^{-/-}$ mice show reduced efficiency of antigen presentation and impaired adaptive cellular immune responses, protecting mice from some autoimmune diseases.[18,26] We therefore quantified leukocyte populations in spleen and lymph nodes of nephritic mice. In contrast to increased leukocyte numbers in the peripheral blood of Ackr2$^{-/-}$ mice (Figure 9b), numbers were not different to those for wild-type mice in both spleen and lymph nodes, including CD4^{+} and CD8^{+} T cells, CD11b^{+}CD11c^{+} dendritic cells, CD11b^{+}F4/80^{+} macrophages, and CD11b^{+}Ly6C^{high} inflammatory macrophages (data not shown). To further investigate whether T-cell activation was impaired in *Ackr2*-deficient mice during autologous NTN, we analyzed surface expression of the activation marker CD69 on CD4^{+} and CD8^{+} T cells isolated from spleens and regional lymph nodes of mice at day 14 of NTN. Our results indicate that systemic T-cell activation in spleen was comparable between wild-type and Ackr2$^{-/-}$ mice, but significantly reduced in regional lymph nodes of *Ackr2*-deficient mice (Figure 11a). Consistently, CD11b^{+}CD11c^{+} dendritic cells in lymph nodes, but not spleens of nephritic Ackr2$^{-/-}$ mice expressed lower levels of the costimulatory molecules CD80 and CD86 (Figure 11b). These data indicate that the influx of activated dendritic cells into draining lymph nodes and subsequent T-cell activation is diminished in nephritic Ackr2$^{-/-}$ mice, despite intact systemic T-cell responses and unaltered total numbers of leukocyte subsets in lymphoid organs. Thus, consistent with previous reports, also in NTN, local adaptive immunity is reduced in *Ackr2*-deficient mice. However, this did not protect Ackr2$^{-/-}$ mice from exacerbated renal inflammation and injury that results from the absent chemokine-scavenging properties of ACKR2 in the renal tubulointerstitium.

DISCUSSION

ACKR2 functions as a chemokine decoy receptor, which can bind, internalize, and degrade a large panel of inflammatory CC chemokines.[27] Therefore, ACKR2 was assumed to play an anti-inflammatory role and regulate resolution of inflammation by chemokine clearance from inflamed sites.[7,26] This was confirmed in several disease models *in vivo*, including skin inflammation, myocardial infarction, systemic infection with *M. tuberculosis*, and toxic liver injury.[13–15,28] In line with these findings, we now show that ACKR2 also plays an important

Figure 5 | Renal leukocyte infiltrates in nephritic wild-type (WT) and *Ackr2*-deficient (Ackr2$^{-/-}$) mice at day 14 of autologous nephrotoxic serum nephritis. (**a**) Flow cytometric analysis of renal single-cell suspensions prepared from nephritic kidneys demonstrated increased leukocyte infiltrates in Ackr2$^{-/-}$ mice compared with WT mice. Cells were stained for CD45 (pan leukocyte marker), CD3 (T lymphocytes), CD3/CD4 (CD4^{+} T helper cells), CD3/CD8 (CD8^{+} cytotoxic T cells), CD11c (dendritic cell-like mononuclear phagocytes), and F4/80 (mononuclear phagocytes). In particular, renal infiltrates of CD3^{+} CD4^{+} T cells and CD11c^{+} F4/80^{+} mononuclear phagocytes significantly increased. Dashed lines indicate mean baseline values for healthy WT mice. (**b**) Representative renal sections of WT and *Ackr2*-deficient mice stained for CD3^{+} T cells, Mac2^{+} glomerular macrophages, and F4/80^{+} interstitial mononuclear phagocytes; original magnification ×400 (glomeruli) (bars = 50 μm), ×200 (tubulointerstitium) (bars = 100 μm). Glomerular and tubulointerstitial leukocyte infiltrates were quantified as described in the Materials and Methods. Data are representative for 2 independent experiments and show mean ± SD of 6 mice per group. *$P < 0.05$, **$P < 0.01$, ***$P < 0.001$. hpf, high power field. To optimize viewing of this image, please see the online version of this article at www.kidney-international.org.

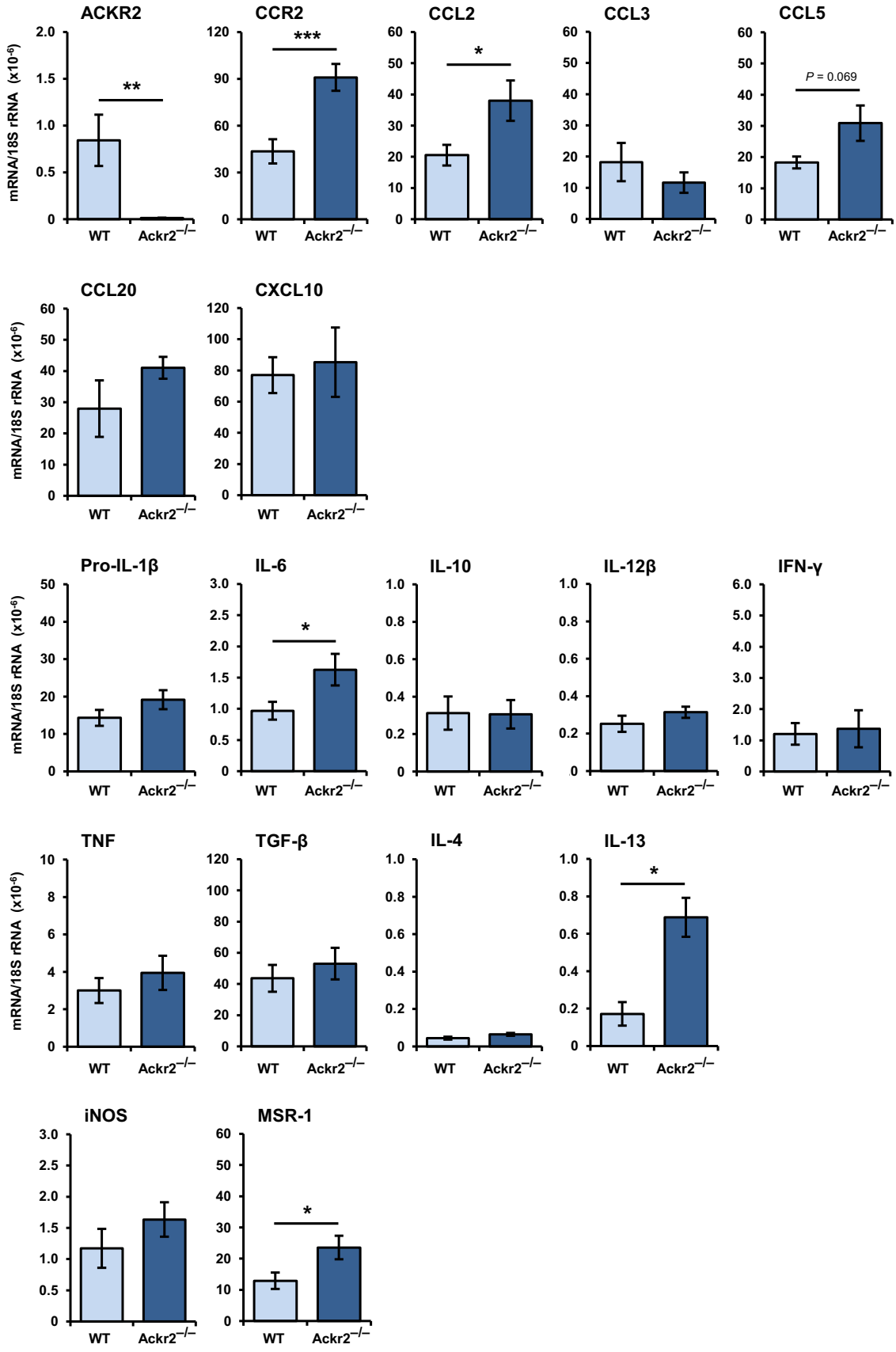

Figure 6| Renal expression of inflammatory markers in nephritic wild-type (WT) and *Ackr2*-deficient (Ackr2$^{-/-}$) mice at day 14 of autologous nephrotoxic serum nephritis. Atypical chemokine receptor 2 (ACKR2) mRNA could not be detected in Ackr2$^{-/-}$ mice. (Continued)

anti-inflammatory role in kidney disease and limits renal injury during progressive immune complex GN. Lack of ACKR2 aggravated functional and structural parameters of renal injury. Increased albuminuria, glomerulosclerosis, glomerular fibrinoid necrosis, and a decreased podocyte count with reduced nephrin expression revealed more severe glomerular damage in *Ackr2*-deficient mice than in wild-type mice. Importantly, elevated serum urea levels, more tubular casts and tubular dilation, increased interstitial volume expansion, and increased renal protein expression of KIM-1 indicated more severe tubulointerstitial injury in Ackr2$^{-/-}$ kidneys. Exacerbated renal injury was paralleled by increased infiltration of leukocytes into nephritic Ackr2$^{-/-}$ kidneys, most prominently CD4^{+} T cells and mononuclear phagocytes, which are important mediators of renal damage in the autologous NTN model.[29,30] Previous studies in disease models including T-cell–dependent ovalbumin-induced lung inflammation,[31] psoriasis-like skin inflammation,[32] and myocardial infarction[14] reported similar findings with increased leukocyte numbers in affected organs of Ackr2$^{-/-}$ mice.

Reduced ability of *Ackr2*-deficient mice to locally degrade proinflammatory chemokines in inflamed tissue may facilitate leukocyte accumulation. We found increased intrarenal levels of the chemokines CCL2 and CCL5 in Ackr2$^{-/-}$ kidneys with NTN, both of which are ACKR2 ligands, which supports this hypothesis. As in other solid organs,[11,14] we could localize renal ACKR2 expression to lymphatic endothelial cells, which in the kidney are present in the tubulointerstitium, but not glomeruli. Consistently, tubulointerstitial cells, but not glomeruli isolated from *Ackr2*-deficient healthy kidneys secreted more CCL2 than wild-type cells did when stimulated with TNF *in vitro*. This suggested that reduced chemokine scavenging by *Ackr2*-deficient lymphatic endothelial cells of the tubulointerstitium increases chemokine levels in nephritic kidneys *in vivo*, independently of subsequent leukocyte infiltration with potential increases in local leukocyte-derived chemokine production. In contrast, CCL2 secretion was comparable in TNF-stimulated glomeruli isolated from healthy Ackr2$^{-/-}$ and wild-type mice, in line with absent lymphatic endothelial cells in glomeruli that could express ACKR2. Consistently, numbers of glomerular T cells and macrophages were similar in both groups of mice with autologous NTN, in contrast to the increased tubulointerstitial accumulation of leukocytes in *Ackr2*-deficient kidneys.

Despite unaltered chemokine scavenging activity and similar leukocyte numbers in glomeruli, *Ackr2* deficiency did result in more severe glomerular damage and albuminuria. Glomerular deposition of immune complexes and complement was comparable in Ackr2$^{-/-}$ and wild-type mice, suggesting similar immune-mediated glomerular injury. Of note, systemic humoral and cellular immune responses were comparable in Ackr2$^{-/-}$ mice, compared with wild-type mice, as shown by autologous antibody serum titers and similar numbers of activated CD69^{+} splenic T cells. In contrast, Ackr2$^{-/-}$ mice showed decreased regional activation of T cells and dendritic cells in draining lymph nodes, indicating compromised adaptive cellular immunity and T-cell priming. These results are again consistent with the expression of ACKR2 on interstitial lymphatic endothelial cells to facilitate efflux of activated antigen-presenting leukocytes into regional lymph nodes.[20,26] This explains why *Ackr2* deletion can be protective in several disease models involving adaptive immunity, including experimental autoimmune encephalitis and graft versus host disease.[18,19] However, immune-mediated glomerular injury in autologous NTN was not ameliorated by *Ackr2* deficiency, most likely due to preserved systemic immune responses.

Exacerbated tubulointerstitial damage, as present in Ackr2$^{-/-}$ mice, can enhance glomerular injury.[3,33] Indeed, it has been shown that targeted tubular injury not only triggers interstitial fibrosis but also glomerulosclerosis and albuminuria.[34] Thus, increased glomerular damage in Ackr2$^{-/-}$ mice may result from exacerbated tubulointerstitial disease. Additionally, as reported previously,[19] *Ackr2* deficiency increased systemic inflammation, characterized by higher circulating CCL2 levels and monocyte numbers in the peripheral blood of Ackr2$^{-/-}$ mice with autologous NTN. CCL2 can directly injure podocytes that express the CCL2 receptor CCR2 and may induce podocyte cell death and increase protein permeability of the glomerular sieve leading to glomerular scaring.[35–39] Thus, chronic exposure of podocytes to elevated systemic CCL2 levels during autologous NTN may contribute to the augmented podocyte loss, which was seen in *Ackr2*-deficient mice, and contribute to exacerbated glomerular injury of Ackr2$^{-/-}$ mice. We additionally investigated Ackr2$^{-/-}$ mice in the heterologous NTN model, which leads to an acute immune complex-mediated GN mediated by innate immune mechanisms.[40] However, neither increased glomerular damage nor more extensive tubulointerstitial leukocyte infiltration and injury were present in Ackr2$^{-/-}$ mice at day 5 of heterologous NTN, despite similarly induced CCL2 levels and elevated numbers of circulating leukocytes as in the chronic autologous model (data not shown). Thus, short-term systemic effects of *Ackr2* deficiency per se do not induce more severe kidney injury in acute GN.

Figure 6 | (Continued) The mRNA expression levels of CC chemokine receptor 2 (CCR2) and its main ligand CCL2 significantly increased in nephritic kidneys of Ackr2$^{-/-}$ mice compared with WT mice, with a similar trend for the proinflammatory chemokines CCL5 and CCL20. In addition, interleukin-6 (IL-6) expression was significantly more abundant in Ackr2$^{-/-}$ kidneys, and a similar trend was noted for IL-1β, tumor necrosis factor (TNF), and transforming growth factor β (TGF-β). Macrophage markers were also more abundantly expressed in *Ackr2*-deficient nephritis kidneys, with a trend for the M1 marker inducible nitric oxide synthase (iNOS) and a significant increase for the M2 marker macrophage scavenger receptor 1 (MSR-1). Data represent mean ± SEM of 10 to 14 mice per group. *$P < 0.05$, **$P < 0.01$, ***$P < 0.001$. CXCL, CXC motif chemokine ligand; IFN, interferon; rRNA, ribosomal RNA.

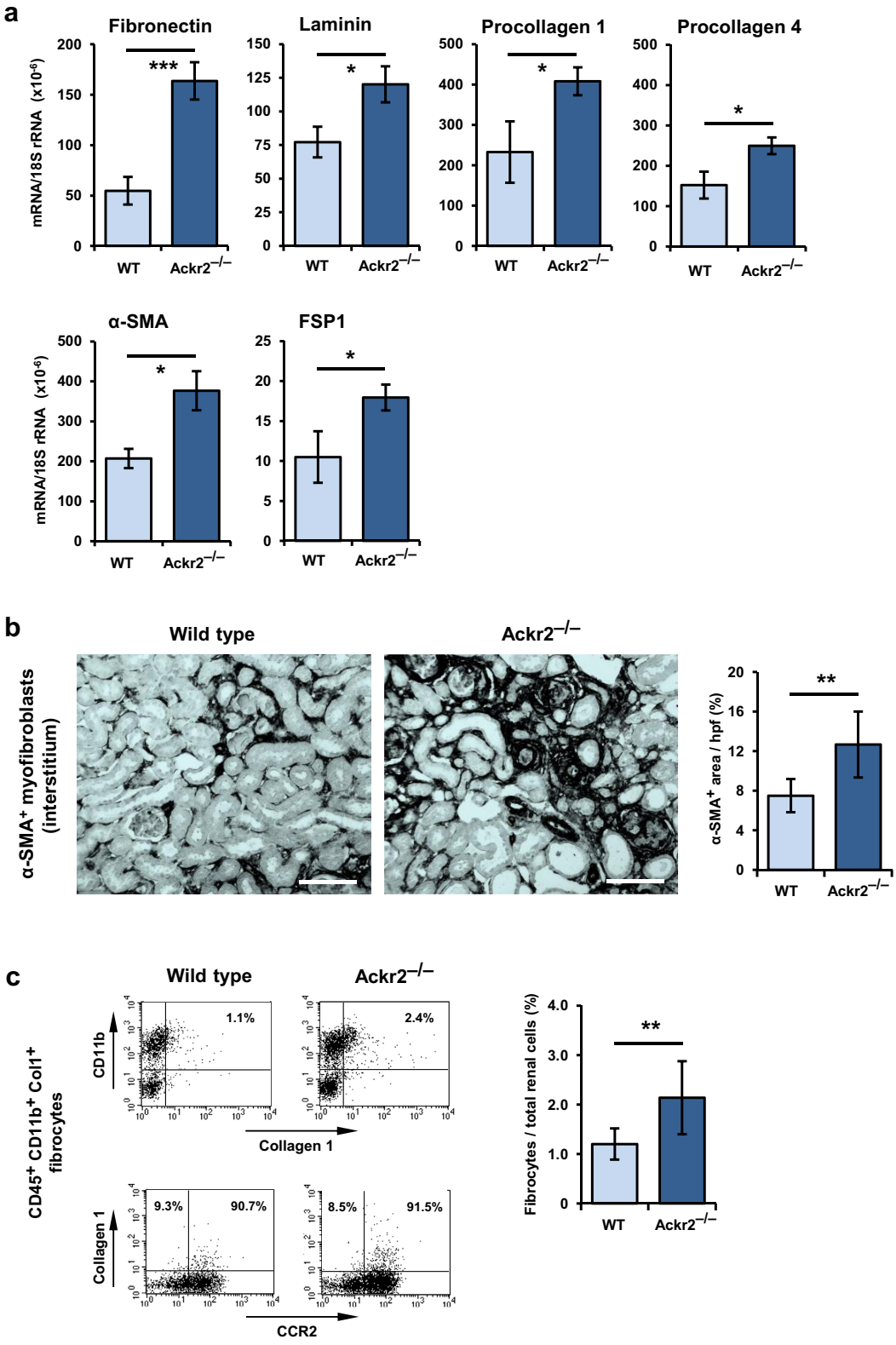

Figure 7 | Markers of renal fibrosis in nephritic wild-type (WT) and *Ackr2*-deficient (Ackr2$^{-/-}$) mice at day 14 of autologous nephrotoxic serum nephritis. (**a**) Markers of fibrotic tissue remodeling were robustly induced in nephritic Ackr2$^{-/-}$ kidneys compared with WT kidneys. Significantly increased mRNA levels of fibronectin, laminin, procollagen 1 and 4, the myofibroblast marker α-smooth muscle actin (α-SMA), and fibroblast-specific protein 1 (FSP1) indicated aggravated renal fibrosis in Ackr2$^{-/-}$mice. Polymerase chain reaction results were normalized to 18S ribosomal RNA (rRNA) as a housekeeping gene. Data represent mean ± SEM of 10 to 14 mice per group. (**b**) Consistently, immunohistology revealed a significantly increased abundance of interstitial α-SMA^{+} myofibroblasts in Ackr2$^{-/-}$ kidneys (original magnification ×200, bars = 100 μm). (**c**) Increased intrarenal accumulation of CD45^{+}CD11b^{+}collagen 1^{+} fibrocytes in nephritic (continued)

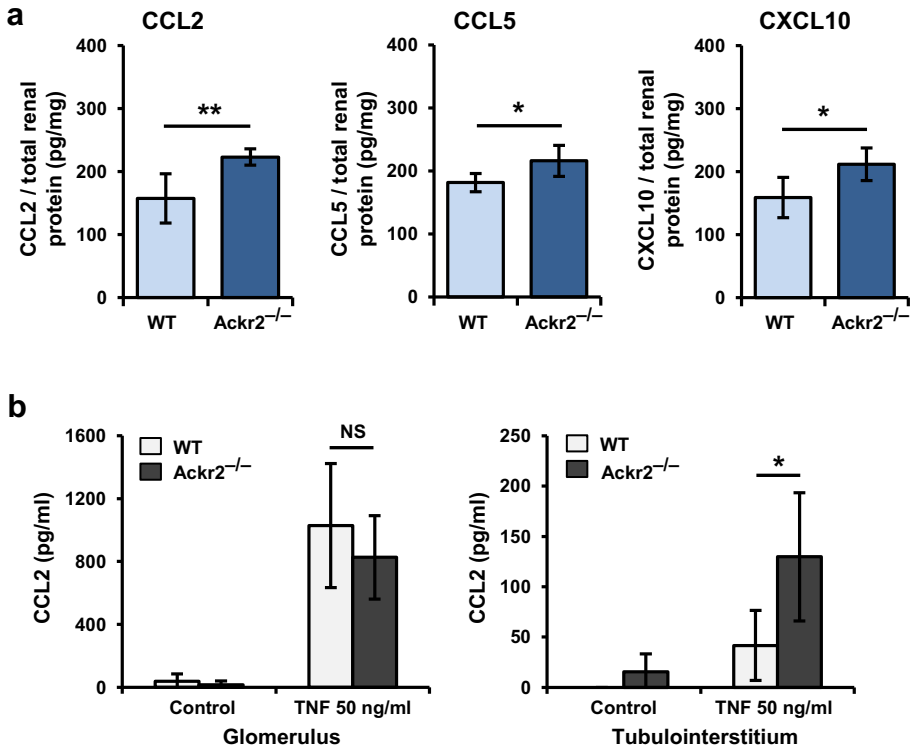

Figure 8 | *Ackr2* deficiency (Ackr2$^{-/-}$) increases renal chemokine levels in inflamed tubulointerstitial tissue. (**a**) Protein levels of the proinflammatory CC chemokine ligand 2 (CCL2), CCL5, and CXC chemokine ligand 10 (CXCL10) were significantly elevated in nephritic kidneys of Ackr2$^{-/-}$ mice at day 14 of nephrotoxic serum nephritis, as measured by enzyme-linked immunosorbent assay of kidney lysates. (**b**) Glomeruli and tubulointerstitial tissue was isolated from healthy wild-type (WT) and Ackr2$^{-/-}$ mice as described in the Materials and Methods. After stimulation with 50 ng/ml tumor necrosis factor (TNF) for 24 hours *in vitro*, CCL2 chemokine levels in the supernatant were measured by enzyme-linked immunosorbent assay. Whereas CCL2 levels were comparable in TNF-stimulated glomeruli of WT and Ackr2$^{-/-}$ mice, TNF-exposed tubulointerstitial tissue of Ackr2$^{-/-}$ mice produced significantly more CCL2 than WT mice did. Data represent mean ± SD of 5 mice per group. *$P < 0.05$, **$P < 0.01$. NS, not significant.

Most strikingly, *Ackr2* deletion resulted not only in increased tubulointerstitial inflammation, but even more pronounced in accelerated fibrotic changes of nephritic kidneys with autologous NTN, as revealed by significantly elevated mRNA expression of major matrix components and a prominent tubulointerstitial accumulation of α-SMA^{+} myofibroblasts. Exacerbated renal fibrosis may result from increased tubulointerstitial cell injury and inflammation in Ackr2$^{-/-}$ kidneys. As renal fibrosis is also mediated by infiltrating CCR2^{+} circulating fibrocytes,[21,22,41] we hypothesized that increased tubulointerstitial CCL2 levels may enhance renal fibrocyte recruitment in *Ackr2*-deficient mice. Respective flow cytometry analysis revealed a significantly greater number of intrarenal CD45^{+}CD11b^{+}collagen 1^{+} fibrocytes in nephritic Ackr2$^{-/-}$ mice compared with wild-type mice. Moreover, in both genotypes renal fibrocytes were largely CCR2-positive. These data are consistent with enhanced CCL2/CCR2-mediated fibrocyte recruitment into *Ackr2*-deficient kidneys contributing to accelerated fibrotic remodeling.

In summary, we demonstrate an important role for ACKR2 in limiting glomerular and tubulointerstitial injury, inflammation, and fibrotic remodeling in progressive immune complex GN due to scavenging of chemokines in the tubulointerstitial compartment. Our data identify ACKR2 as a potential target for therapeutic approaches in renal inflammatory and fibrotic disease. Such therapies could include enhanced systemic scavenging of proinflammatory chemokines utilizing ACKR2-IgG fusion proteins similar to TNF blockade with etanercept. More elegantly, renal ACKR2

Figure 7 | (continued) Ackr2$^{-/-}$ kidneys compared with WT kidneys as quantified by flow cytometry. Representative dot plots gated on CD45^{+} renal cells are shown for nephritic WT and Ackr2$^{-/-}$ mice at day 14 of nephrotoxic nephritis (upper panel). Numbers represent the mean fibrocyte count per total renal cell count of each genotype. In both genotypes, CC chemokine receptor 2 (CCR2) surface expression was present in most renal fibrocytes (lower panel, gated on CD11b^{+} renal cells). Numbers illustrate the mean percentages of CCR2-negative and CCR2-positive CD11b^{+}collagen 1^{+} fibrocytes in each genotype. Data represent mean ± SD of 6 mice per group. *$P < 0.05$, ** $P < 0.01$, ***$P < 0.001$. hpf, high-power field. To optimize viewing of this image, please see the online version of this article at www.kidney-international.org.

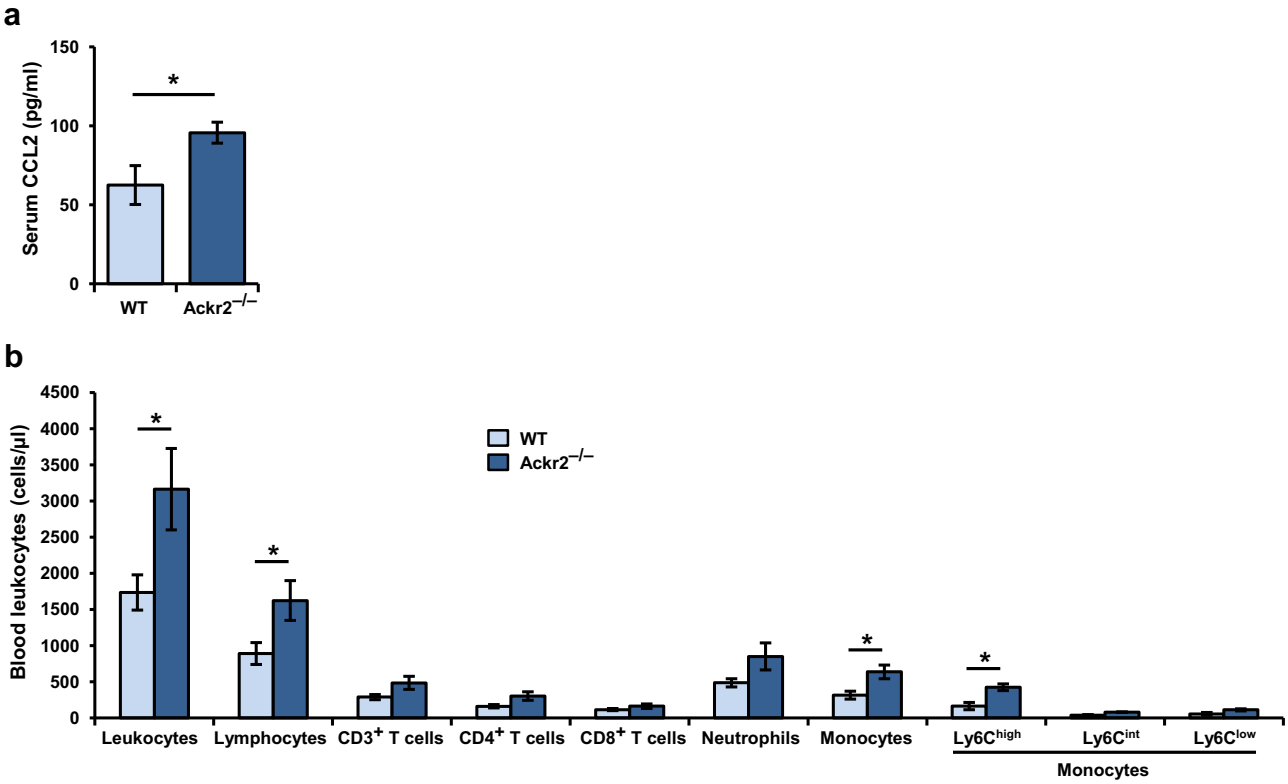

Figure 9 | Serum levels of CC chemokine ligand 2 (CCL2) and peripheral blood leukocyte counts in nephritic wild-type (WT) and *Ackr2*-deficient (Ackr2$^{-/-}$) mice at day 14 of autologous nephrotoxic serum nephritis. (**a**) CCL2 concentrations in the serum significantly increased in Ackr2$^{-/-}$ mice with autologous nephrotoxic nephritis at day 14. Data represent mean ± SEM of 5 to 7 mice per group. (**b**) Flow cytometric analysis of whole blood revealed a significant increase in circulating leukocytes, including lymphocytes and inflammatory Ly6C^{high} monocytes in *Ackr2*-deficient mice with autologous nephrotoxic nephritis at day 14. Data represent mean ± SEM of 10 to 12 mice per group. *$P < 0.05$.

expression may be augmented with mRNA stabilizing compounds specifically delivered to the renal tubulointerstitium.[42]

MATERIALS AND METHODS

Mice

Ackr2-deficient mice on the C57BL/6J background have been described previously[15,32] and were originally provided by Massimo Locati (Humanitas Clinical and Research Center, Rozzano, Italy). Knockout mice underwent embryo transfer to meet general standards of our institution. All experiments were performed in 7- to 9-week-old male *Ackr2*$^{-/-}$ mice and wild-type littermate control mice. Genotyping of mice was performed as described.[32] All experimental procedures were performed according to the German animal care and ethics legislation and had been approved by the local government authorities.

Induction of autologous NTN

Autologous NTN was induced as reported previously[40] by injecting 50 µl of a commercially available sheep nephrotoxic serum (Probetex, San Antonio, TX) in the tail vein of presensitized mice that had been immunized subcutaneously in both flanks with 20 µg of sheep IgG (Jackson ImmunoResearch Labs, West Grove, PA) 3 days earlier. At day 14, mice were killed, peripheral blood was collected by retroorbital bleeding and perfused kidneys, spleen, and lymph nodes were harvested for histological analysis, flow cytometry, mRNA, and protein detection.

Functional assessment of renal injury

Urinary albumin-creatinine ratios (mg/mg) in spot urine samples were determined as described.[43] Serum values for urea were measured with an Olympus AU-640 auto-analyzer (Tokyo, Japan) at Synlab.vet (Augsburg, Germany).

Assessment of glomerular and tubulointerstitial injury by histology and immunohistochemistry

Renal injury was evaluated on 2-µm formalin-fixed, paraffin-embedded renal sections. The extent of glomerular matrix deposition was semiquantitatively scored on periodic acid-Schiff (PAS)-stained sections as follows: grade 0, no PAS-positive material; grade 1, ≤25% of glomerular cross-section is positive; grade 2, 26% to 50% is positive; grade 3, 51% to 75% is positive; and grade 4, ≥76% is positive. Fifty glomeruli per mouse were scored and the mean glomerular matrix score was calculated for each mouse. The extent of glomerular fibrinoid necrosis was assessed after immunohistochemical staining with polyclonal rabbit anti-mouse fibrinogen (1:500, Abcam, Cambridge, UK) and quantified with ImageJ (National Institutes of Health, Bethesda, MD). Glomerular podocyte counts were determined after immunofluorescence staining for nephrin and Wilms tumor antigen-1 as previously described.[44] The extent of glomerular nephrin expression was quantified by determining the area of positive nephrin staining per glomerular tuft area in 40 glomeruli per mouse using ImageJ. Tubulointerstitial injury was evaluated on PAS-stained sections in 10 cortical high-power fields per mouse by quantifying tubular casts, and by

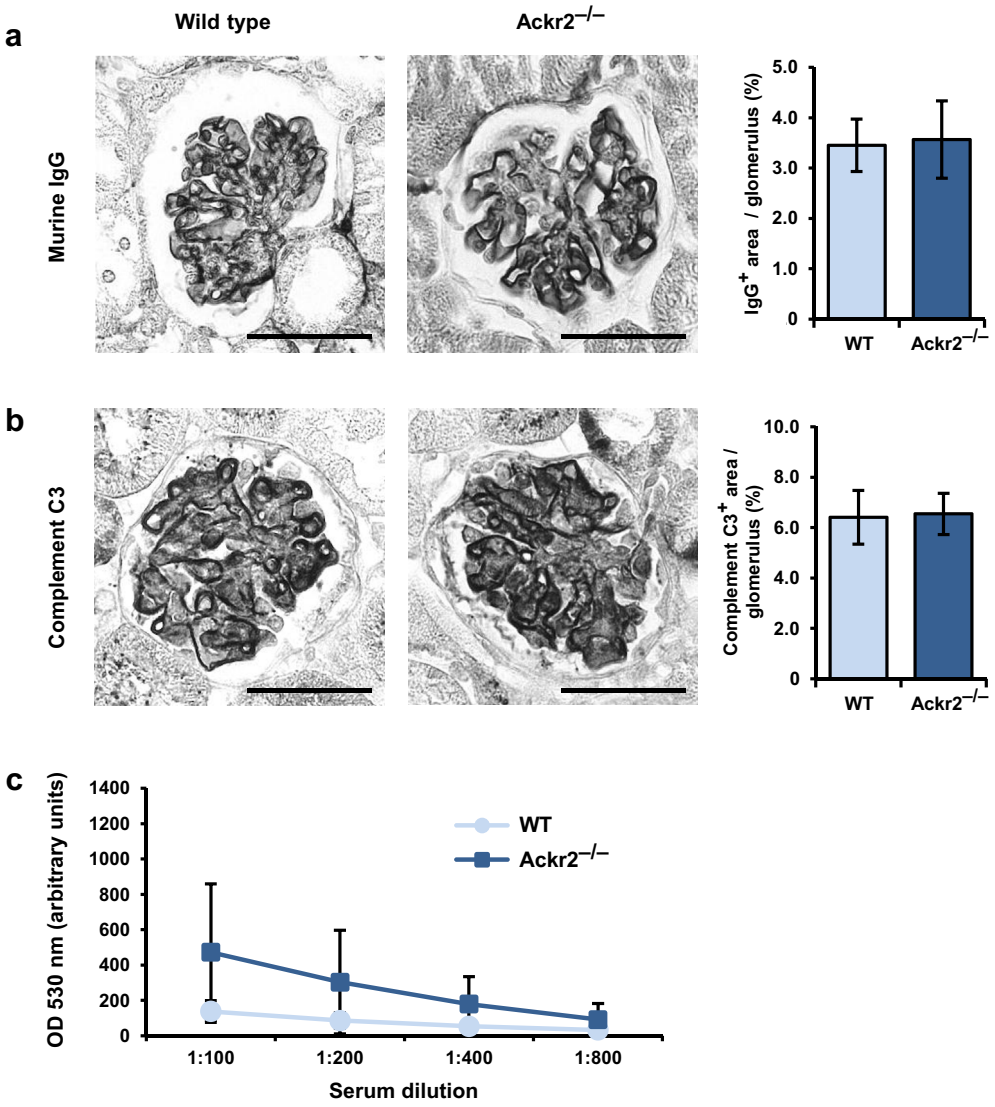

Figure 10 | Humoral immune response in wild-type (WT) and *Ackr2*-deficient (Ackr2$^{-/-}$) mice at day 14 of autologous nephrotoxic serum nephritis. Representative photomicrographs of glomerular sections from WT and Ackr2$^{-/-}$ mice after immunohistochemical staining for murine IgG (**a**) and complement C3 (**b**). Quantitative assessment revealed similar glomerular deposition of autologous IgG and C3 in both genotypes. Original magnification ×400, bars = 50 μm. Data represent mean ± SD of 5 mice per group. (**c**) Autologous murine anti-sheep antibody levels were determined by enzyme-linked immunosorbent assay from serum samples on day 14 of nephrotoxic nephritis. Titers in serial dilutions of serum are expressed in arbitrary units. OD 530, optical density at 530 nm. To optimize viewing of this image, please see the online version of this article at www.kidney-international.org.

semiquantitative scoring of tubular dilation and interstitial volume expansion in a range of 0 to 3. The extent of tubulointerstitial fibroblast accumulation was quantified by measuring positive staining for α-SMA (1:300, clone 1A4, DAKO Agilent, Santa Clara, CA) in 10 cortical high-power fields per mouse.

RNA *in situ* hybridization combined with immunofluorescence

Before RNAscope assay application (Advanced Cell Diagnostics, Hayward, CA), 5-μm paraffin sections were baked in a dry oven at 60°C for 1 hour. The probe for murine Ackr2 mRNA was developed by Advanced Cell Diagnostics. Ackr2 mRNA was localized using the RNAscope 2.5 HD reagent kit "Red" (Advanced Cell Diagnostics) as detection reagent. Consecutively, lymphatic endothelium was stained with polyclonal anti-LYVE-1 antibody (AngioBio, Del Mar, CA). LYVE-1 was displayed by the tyramide signal amplification method (TSA kit, streptavidin coupled to AF 488; Invitrogen/Molecular Probes, Thermo Fisher Scientific, Schwerte, Germany).

Flow cytometry and immunohistochemistry for renal and peripheral blood leukocytes

Preparation of renal single-cell suspensions and antibody staining were performed as described previously.[45–47] Intrarenal fibrocytes were identified by surface staining for CD45 and CD11b, followed by intracellular staining with biotinylated anti-collagen 1 or respective isotype control (Rockland Immunochemicals, Gilbertsville, PA) as published.[22] For CCR2 surface staining, rat anti-mouse CCR2 (clone #475301) and isotype control (R&D Systems, Abingdon, UK) were used. Analysis was done with a FACSCalibur flow cytometer and Cellquest software (BD Biosciences, Heidelberg, Germany). The number of stained renal leukocytes was expressed as percentage of

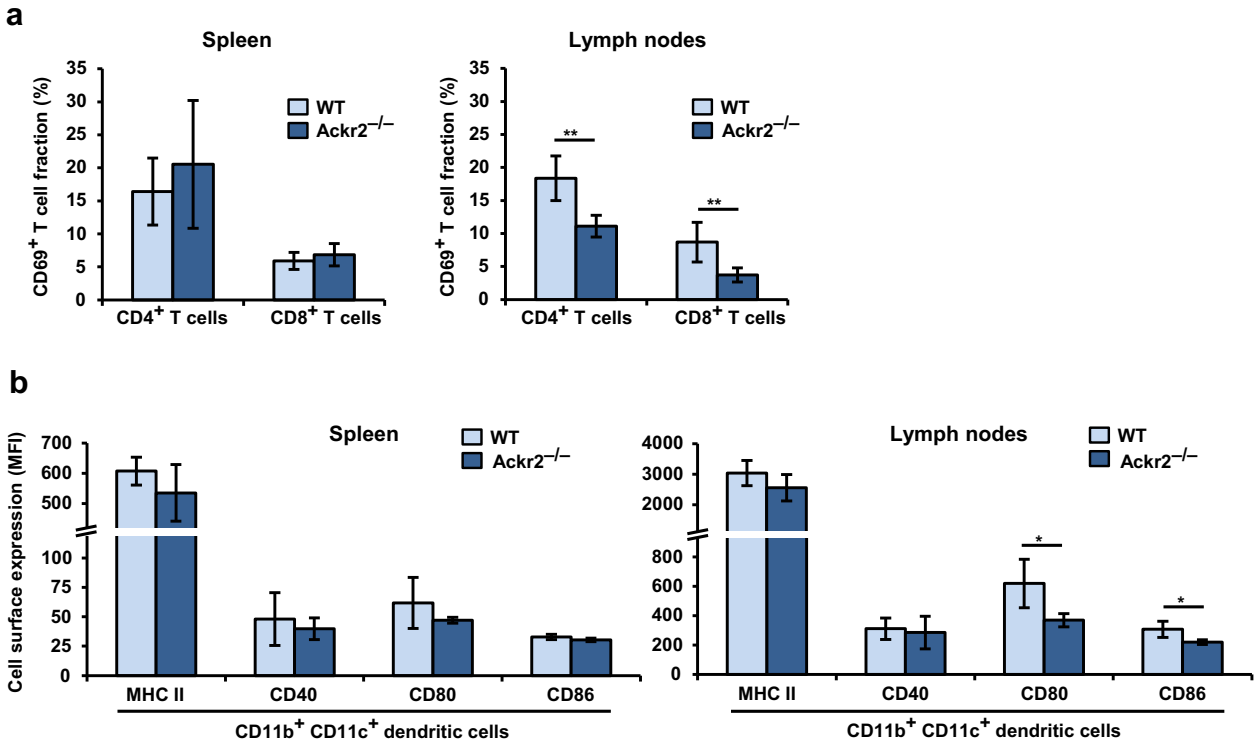

Figure 11 | Systemic and regional activation of T cells and dendritic cells in wild-type (WT) and *Ackr2*-deficient (Ackr2$^{-/-}$) mice at day 14 of autologous nephrotoxic serum nephritis. (**a**) The fraction of activated CD3$^+$CD4$^+$ and CD3$^+$CD8$^+$ T cells in spleens and regional lymph nodes of nephritic mice with nephrotoxic nephritis were determined by flow cytometric analysis of CD69 surface staining. CD69 expression was comparable in splenic T cells, but significantly reduced in T cells of regional lymph nodes isolated from Ackr2$^{-/-}$ mice. (**b**) Dendritic cells were identified as CD45$^+$CD11b$^+$CD11c$^+$ cells, and expression of surface markers major histocompatibility complex II (MHC II), CD40, CD80, and CD86 was analyzed. In dendritic cells of lymph nodes, but not spleen, expression of the costimulatory molecules CD80 and CD86 was significantly lower in Ackr2$^{-/-}$ mice compared with WT mice, as revealed by decreased mean fluorescence intensities (MFI). Data represent mean ± SD of 5 mice per group. *$P < 0.05$, **$P < 0.01$.

total renal cells. Peripheral blood leukocytes were quantified adding counting beads (Molecular Probes, Eugene, OR).

For compartment-specific evaluation of renal leukocyte infiltrates, 2-μm paraffin-embedded renal sections were stained with primary antibodies against CD3$^+$ T cells (cross-reactive rat anti-human CD3, 1:100, clone CD3-12, Abd Serotec, Oxford, UK) and mononuclear phagocytes (rat anti-mouse Mac 2, clone M3/38, 1:3.000; rat anti-mouse F4/80, clone Cl:A3-1, 1:100, both from Abd Serotec) as previously described.[45] Stained cells were counted in 50 glomeruli and 20 cortical high-power fields per mouse. F4/80-positive infiltrates in the tubulointerstitium were quantified as the fraction of stained area using ImageJ. All assessments were performed in a blinded protocol.

Quantitative reverse transcriptase polymerase chain reaction

Total RNA was extracted from whole kidneys using the Purelink RNA Mini Kit (Ambion, Foster City, CA). SYBR Green master mix (Invitrogen, Carlsbad, CA) was used to perform real-time quantitative reverse transcriptase polymerase chain reaction on a Light Cycler 480 (Roche, Mannheim, Germany). All used primers (Metabion, Martinsried, Germany) are listed in Table 1. All samples were run in duplicate and normalized to 18s ribosomal RNA.

Analysis of humoral and cellular immune responses

Serum levels of autologous mouse anti-sheep IgG were measured by enzyme-linked immunosorbent assay (ELISA) as previously described.[45] Glomerular disposition of murine IgG and complement C3 were determined after staining paraffin-embedded sections with goat-anti-mouse IgG antibody (clone BA-9200, 1:400, Vector, Burlingame, CA) and polyclonal rabbit anti-mouse C3c (1:100, Biorbyt, Cambridge, UK), respectively. Positive staining in 15 glomeruli per mouse was quantified by ImageJ. Systemic and local activation of T cells and dendritic cells at day 14 of NTN was characterized by flow cytometry measuring expression of the activation marker CD69 on CD4$^+$ and CD8$^+$ T cells, and of major histocompatibility complex II (I-A^b), CD40, CD80, and CD86 on CD11b$^+$CD11c$^+$ dendritic cells isolated from spleen and regional lymph nodes.

Analysis of KIM-1 and chemokine protein levels by ELISA

Total kidney lysates were prepared from mice at day 14 of NTN. Renal KIM-1 expression and chemokine levels in total kidney lysates and serum were determined using commercially available ELISA kits for KIM-1, CCL2, CCL5, and CXCL10 (R&D Systems) following the manufacturer's protocols. Protein content of each kidney sample was normalized using Bradford protein assay.

Separation and stimulation of glomeruli and tubulointerstitial tissue

To separate glomeruli and tubulointerstitial tissue from normal mouse kidney, a magnetic bead-based isolation method was adapted from Takemoto *et al.*,[48] and performed as previously described in detail.[46] A total of 10,000 glomeruli and 100 μl of tubulointerstitial cell suspensions standardized to a protein content of 0.5 mg/ml were incubated in 3 ml Roswell Park Memorial Institution 1640 medium

Table 1 | Primers used for real-time qRT-PCR

Gene target	Primer sequence
Nephrin	5′-ACCCTCCAGTTAACTTGTCTTTGG-3′ (forward), 5′-ATGCAGCGGAGCCTTTGA-3′ (reverse)
ACKR2	5′-CTTCTTTTACTCCCGCATCG-3′ (forward), 5′-TATGGGAACCACAGCATGAA-3′ (reverse)
CCR2	5′-GGGCATTGGATTCACCAC-3′ (forward), 5′-CCGTGGATGAACTGAGGTAAC-3′ (reverse)
CCL2	5′-CCTGCTGTTCACAGTTGCC-3′ (forward), 5′-ATTGGGATCATCTTGCTGGT-3′ (reverse)
CCL3	5′-CATATGGAGCTGACACCCCG -3′ (forward), 5′- CAGGAAAATGACACCTGGCTG -3′ (reverse)
CCL5	5′-CCACTTCTTCTCTGGGTTGG-3′ (forward), 5′-GTGCCCACGTCAAGGAGTAT-3′ (reverse)
CCL20	5′-TCTGCTCTTCCTTGCTTTGG-3′ (forward), 5′-TGTACGAGAGGCAACAGTCG-3′ (reverse)
CXCL10	5′-GGCTGGTCACCTTTCAGAAG-3′ (forward), 5′-ATGGATGGACAGCAGAGAGC-3′ (reverse)
pro-IL-1β	5′-TTCCTTGTGCAAGTGTCTGAAG-3′ (forward), 5′-CACTGTCAAAAGGTGGCATTT-3′ (reverse)
IL-4	5′-TGAACGAGGTCACAGGAGAA-3′ (forward), 5′-CGAGCTCACTCTCTGTGGTG-3′ (reverse)
IL-6	5′-TGATGCACTTGCAGAAAACA-3′ (forward), 5′-ACCAGAGGAAATTTTCAATAGGC-3′ (reverse)
IL-10	5′-ATCGATTTCTCCCCTGTGAA-3′ (forward), 5′-TGTCAAATTCATTCATGGCCT-3′ (reverse)
IL-12β	5′-GATTCAGACTCCAGGGGACA-3′ (forward), 5′-GGAGACACCAGCAAAACGAT-3′ (reverse)
IL-13	5′-ACATCACACAAGACCAGACTCC-3′ (forward), 5′-GAGGCCATGCAATATCCTCT-3′ (reverse)
IFN-γ	5′-ACAGCAAGGCGAAAAAGGAT-3′ (forward), 5′-TGAGCTCATTGAATGCTTGG-3′ (reverse)
TNF	5′-CCACCACGCTCTTCTGTCTAC-3′ (forward), 5′-AGGGTCTGGGCCATAGAACT-3′ (reverse)
TGF-β	5′-GGAGAGCCCTGGATACCAAC-3′ (forward), 5′-CAACCCAGGTCCTTCCTAAA-3′ (reverse)
iNOS1	5′-TTCTGTGCTGTCCCAGTGAG-3′ (forward), 5′-TGAAGAAAACCCCTTGTGCT-3′ (reverse)
MSR-1	5′-CCTCCGTTCAGGAGAAGTTG-3′ (forward), 5′-TTTCCCAATTCAAAAGCTGA-3′ (reverse)
Fibronectin	5′-GGAGTGGCACTGTCAACCTC-3′ (forward), 5′-ACTGGATGGGGTGGGAAT-3′ (reverse)
Laminin	5′-CATGTGCTGCCTAAGGATGA-3′ (forward), 5′-TCAGCTTGTAGGAGATGCCA-3′ (reverse)
Procollagen 1α1	5′-ACATGTTCAGCTTTGTGGACC-3′ (forward), 5′-TAGGCCATTGTGTATGCAGC-3′ (reverse)
Procollagen 4α1	5′-GTCTGGCTTCTGCTGCTCTT-3′ (forward), 5′-CACATTTTCCACAGCCAGAG-3′ (reverse)
α-SMA	5′-ACTGGGACGACATGGAAAAG-3′ (forward), 5′-GTTCAGTGGTGCCTCTGTCA-3′ (reverse)
FSP1	5′-CAGCACTTCCTCTCTCTTGG-3′ (forward), 5′-TTTGTGGAAGGTGGACACAA-3′ (reverse)

ACKR, atypical chemokine receptor; CCL, CC chemokine ligand; CCR, CC chemokine receptor; CXCL, CXC chemokine ligand; FSP; fibroblast specific protein; IFN, interferon; IL, interleukin; iNOS, inducible nitric oxide synthase; MSR, macrophage scavenger receptor; qRT-PCR, quantitative reverse transcriptase polymerase chain reaction; SMA; smooth muscle actin; TGF, transforming growth factor; TNF, tumor necrosis factor.

supplemented with 15% fetal calf serum, 15 mmol/l *N*-2-hydroxyethylpiperazine-*N*′ -2-ethanesulfonic acid buffer, 0.66 U/ml insulin, and penicillin-streptomycin at 37°C for 24 hours. After serum starving for additional 24 hours, tissue was stimulated with 50 ng/ml recombinant murine TNF in Roswell Park Memorial Institution 1640 for 24 hours. CCL2 levels in supernatants were determined by ELISA.

Statistical analysis

Results are presented as mean ± SD or SEM as indicated. Differences between 2 experimental groups were compared with 2-tailed *t*-test, and $P < 0.05$ was considered significant.

DISCLOSURE

All the authors declared no competing interests.

ACKNOWLEDGMENTS

The expert technical assistance of Dan Draganovici and Jana Mandelbaum is gratefully acknowledged. This study was supported by grants from the Medical Faculty of the Ludwig-Maximilians-University Munich to AB and VV and from the Deutsche Forschungsgemeinschaft DFG (VI 231/3-1) to VV. Portions of this work were prepared by AB as part of his doctoral thesis at the Faculty of Medicine, Ludwig-Maximilians-University Munich. A part of the results was presented previously in abstract form (Bideak A, Vielhauer V. Function of the atypical chemokine receptor 2 in murine immune complex glomerulonephritis. *J Am Soc Nephrol*. 2016;27:126A).

REFERENCES

1. Chadban SJ, Atkins RC. Glomerulonephritis. *Lancet*. 2005;365:1797–1806.
2. Kurts C, Panzer U, Anders HJ, et al. The immune system and kidney disease: basic concepts and clinical implications. *Nat Rev Immunol*. 2013;13:738–753.
3. Kurts C, Heymann F, Lukacs-Kornek V, et al. Role of T cells and dendritic cells in glomerular immunopathology. *Semin Immunopathol*. 2007;29:317–335.
4. Rot A, von Andrian UH. Chemokines in innate and adaptive host defense: basic chemokinese grammar for immune cells. *Annu Rev Immunol*. 2004;22:891–928.
5. Zlotnik A, Yoshie O. Chemokines: a new classification system and their role in immunity. *Immunity*. 2000;12:121–127.
6. Mantovani A, Bonecchi R, Locati M. Tuning inflammation and immunity by chemokine sequestration: decoys and more. *Nat Rev Immunol*. 2006;6:907–918.
7. Graham GJ, Locati M. Regulation of the immune and inflammatory responses by the "atypical" chemokine receptor D6. *J Pathol*. 2013;229:168–175.
8. Nibbs RJ, Graham GJ. Immune regulation by atypical chemokine receptors. *Nat Rev Immunol*. 2013;13:815–829.
9. Nibbs RJ, Wylie SM, Pragnell IB, et al. Cloning and characterization of a novel murine beta chemokine receptor, D6: comparison to three other related macrophage inflammatory protein-1alpha receptors, CCR-1, CCR-3, and CCR-5. *J Biol Chem*. 1997;272:12495–12504.
10. Nibbs RJ, Wylie SM, Yang J, et al. Cloning and characterization of a novel promiscuous human beta-chemokine receptor D6. *J Biol Chem*. 1997;272:32078–32083.
11. Nibbs RJ, Kriehuber E, Ponath PD, et al. The beta-chemokine receptor D6 is expressed by lymphatic endothelium and a subset of vascular tumors. *Am J Pathol*. 2001;158:867–877.
12. Rot A, McKimmie C, Burt CL, et al. Cell-autonomous regulation of neutrophil migration by the D6 chemokine decoy receptor. *J Immunol*. 2013;190:6450–6456.
13. Martinez de la Torre Y, Locati M, Buracchi C, et al. Increased inflammation in mice deficient for the chemokine decoy receptor D6. *Eur J Immunol*. 2005;35:1342–1346.
14. Cochain C, Auvynet C, Poupel L, et al. The chemokine decoy receptor D6 prevents excessive inflammation and adverse ventricular remodeling after myocardial infarction. *Arterioscler Thromb Vasc Biol*. 2012;32:2206–2213.
15. Di Liberto D, Locati M, Caccamo N, et al. Role of the chemokine decoy receptor D6 in balancing inflammation, immune activation, and antimicrobial resistance in Mycobacterium tuberculosis infection. *J Exp Med*. 2008;205:2075–2084.
16. Nibbs RJ, Gilchrist DS, King V, et al. The atypical chemokine receptor D6 suppresses the development of chemically induced skin tumors. *J Clin Invest*. 2007;117:1884–1892.
17. Vetrano S, Borroni EM, Sarukhan A, et al. The lymphatic system controls intestinal inflammation and inflammation-associated colon

cancer through the chemokine decoy receptor D6. *Gut*. 2010;59:197–206.
18. Liu L, Graham GJ, Damodaran A, et al. Cutting edge: the silent chemokine receptor D6 is required for generating T cell responses that mediate experimental autoimmune encephalomyelitis. *J Immunol*. 2006;177:17–21.
19. Savino B, Castor MG, Caronni N, et al. Control of murine Ly6C(high) monocyte traffic and immunosuppressive activities by atypical chemokine receptor D6. *Blood*. 2012;119:5250–5260.
20. Lee KM, McKimmie CS, Gilchrist DS, et al. D6 facilitates cellular migration and fluid flow to lymph nodes by suppressing lymphatic congestion. *Blood*. 2011;118:6220–6229.
21. Niedermeier M, Reich B, Rodriguez Gomez M, et al. CD4+ T cells control the differentiation of Gr1+ monocytes into fibrocytes. *Proc Natl Acad Sci U S A*. 2009;106:17892–17897.
22. Reich B, Schmidbauer K, Rodriguez Gomez M, et al. Fibrocytes develop outside the kidney but contribute to renal fibrosis in a mouse model. *Kidney Int*. 2013;84:78–89.
23. Serbina NV, Pamer EG. Monocyte emigration from bone marrow during bacterial infection requires signals mediated by chemokine receptor CCR2. *Nat Immunol*. 2006;7:311–317.
24. Li L, Huang L, Sung SS, et al. The chemokine receptors CCR2 and CX3CR1 mediate monocyte/macrophage trafficking in kidney ischemia-reperfusion injury. *Kidney Int*. 2008;74:1526–1537.
25. Rosenkranz AR, Knight S, Sethi S, et al. Regulatory interactions of ab and gd T cells in glomerulonephritis. *Kidney Int*. 2000;58:1055–1066.
26. Lee KM, Nibbs RJ, Graham GJ. D6: the "crowd controller" at the immune gateway. *Trends Immunol*. 2013;34:7–12.
27. Weber M, Blair E, Simpson CV, et al. The chemokine receptor D6 constitutively traffics to and from the cell surface to internalize and degrade chemokines. *Mol Biol Cell*. 2004;15:2492–2508.
28. Berres ML, Trautwein C, Zaldivar MM, et al. The chemokine scavenging receptor D6 limits acute toxic liver injury in vivo. *Biol Chem*. 2009;390:1039–1045.
29. Tipping PG, Huang XR, Qi M, et al. Crescentic glomerulonephritis in CD4- and CD8-deficient mice: requirement for CD4 but not CD8 cells. *Am J Pathol*. 1998;152:1541–1548.
30. Duffield JS. Selective depletion of macrophages reveals distinct, opposing roles during liver injury and repair. *J Clin Invest*. 2005;115:56–65.
31. Whitehead GS, Wang T, DeGraff LM, et al. The chemokine receptor D6 has opposing effects on allergic inflammation and airway reactivity. *Am J Respir Crit Care Med*. 2007;175:243–249.
32. Jamieson T, Cook DN, Nibbs RJ, et al. The chemokine receptor D6 limits the inflammatory response in vivo. *Nat Immunol*. 2005;6:403–411.
33. Hochheiser K, Engel DR, Hammerich L, et al. Kidney dendritic cells become pathogenic during crescentic glomerulonephritis with proteinuria. *J Am Soc Nephrol*. 2011;22:306–316.
34. Grgic I, Campanholle G, Bijol V, et al. Targeted proximal tubule injury triggers interstitial fibrosis and glomerulosclerosis. *Kidney Int*. 2012;82:172–183.
35. Burt D, Salvidio G, Tarabra E, et al. The monocyte chemoattractant protein-1/cognate CC chemokine receptor 2 system affects cell motility in cultured human podocytes. *Am J Pathol*. 2007;171:1789–1799.
36. Lee EY, Chung CH, Khoury CC, et al. The monocyte chemoattractant protein-1/CCR2 loop, inducible by TGF-β, increases podocyte motility and albumin permeability. *Am J Physiol Renal Physiol*. 2009;297:F85–F94.
37. Tarabra E, Giunti S, Barutta F, et al. Effect of the monocyte chemoattractant protein-1/CC chemokine receptor 2 system on nephrin expression in streptozotocin-treated mice and human cultured podocytes. *Diabetes*. 2009;58:2109–2118.
38. Nam BY, Paeng J, Kim SH, et al. The MCP-1/CCR2 axis in podocytes is involved in apoptosis induced by diabetic conditions. *Apoptosis*. 2012;17:1–13.
39. You H, Gao T, Raup-Konsavage WM, et al. Podocyte-specific chemokine (C-C motif) receptor 2 overexpression mediates diabetic renal injury in mice. *Kidney Int*. 2017;91:671–682.
40. Hoppe JM, Vielhauer V. Induction and analysis of nephrotoxic serum nephritis in mice. *Methods Mol Biol*. 2014;1169:159–174.
41. Xia Y, Entman ML, Wang Y. CCR2 regulates the uptake of bone marrow-derived fibroblasts in renal fibrosis. *PLoS One*. 2013;8:e77493.
42. Feigerlova E, Battaglia-Hsu SF. Role of post-transcriptional regulation of mRNA stability in renal pathophysiology: focus on chronic kidney disease. *FASEB J*. 2017;31:457–468.
43. Vielhauer V, Berning E, Eis V, et al. CCR1 blockade reduces interstitial inflammation and fibrosis in mice with glomerulosclerosis and nephrotic syndrome. *Kidney Int*. 2004;66:2264–2278.
44. Ryu M, Mulay SR, Miosge N, et al. Tumour necrosis factor-alpha drives Alport glomerulosclerosis in mice by promoting podocyte apoptosis. *J Pathol*. 2012;226:120–131.
45. Vielhauer V, Allam R, Lindenmeyer MT, et al. Efficient renal recruitment of macrophages and T cells in mice lacking the duffy antigen/receptor for chemokines. *Am J Pathol*. 2009;175:119–131.
46. Schwarz M, Taubitz A, Eltrich N, et al. Analysis of TNF-mediated recruitment and activation of glomerular dendritic cells in mouse kidneys by compartment-specific flow cytometry. *Kidney Int*. 2013;84:116–129.
47. Andersen K, Eltrich N, Lichtnekert J, et al. The NLRP3/ASC inflammasome promotes T-cell-dependent immune complex glomerulonephritis by canonical and noncanonical mechanisms. *Kidney Int*. 2014;86:965–978.
48. Takemoto M, Asker N, Gerhardt H, et al. A new method for large scale isolation of kidney glomeruli from mice. *Am J Pathol*. 2002;161:799–805.